Monte Carlo method for modeling of small signal response including the Pauli exclusion principle

S. Smirnov,[a] H. Kosina, M. Nedjalkov, and S. Selberherr
Institute for Microelectronics, TU Vienna, Gusshausstrasse 27-29, A-1040 Vienna, Austria

(Received 25 June 2003; accepted 15 August 2003)

A Monte Carlo method for small signal analysis of degenerate semiconductors is presented. The response to an electric field impulse parallel to the stationary electric field is obtained using the nonlinear Boltzmann kinetic equation with the Pauli exclusion principle in the scattering operator. After linearization of the Boltzmann equation a new Monte Carlo algorithm for small signal analysis of the nonlinear Boltzmann kinetic equation is constructed using an integral representation of the first order equation. The generation of initial distributions for two carrier ensembles which arise in the method is performed by simulating a main trajectory to solve the zero order equation. The normalization of the static distribution function is discussed. To clarify the physical interpretation of our algorithm we consider the limiting case of vanishing electric field and show that in this case kinetic processes are determined by a linear combination of forward and backward scattering rates. It is shown that at high degeneracy backward scattering processes are dominant, while forward transitions are quantum mechanically forbidden under such conditions due to the Pauli exclusion principle. Finally, the small signal Monte Carlo algorithm is formulated and the results obtained for degenerate semiconductors are discussed. © *2003 American Institute of Physics.*
[DOI: 10.1063/1.1616982]

I. INTRODUCTION

To investigate the small signal response of the carriers in semiconductors, different Monte Carlo techniques are widely applied to solve the time-dependent Boltzmann equation.[1–5] There are also small signal approaches based on the velocity and energy balance equations.[6] However, a significant advantage of Monte Carlo methods based on the Boltzmann kinetic equation is that they allow a comprehensive treatment of kinetic phenomena within the quasiclassical approach and account, in a rather simple way, for accurate band structures. Additionally, the quantum mechanical Pauli exclusion principle can be taken into consideration to study the small signal response of carriers in degenerate semiconductors.

When the carrier density is very high the Pauli exclusion principle becomes important and may have a strong influence on different differential response functions which relate a small perturbation of the electric field and a mean value of some physical quantity. The influence is expected to be strong and it has been pointed out[4] that the behavior of impulse response functions is determined by the overlap of the distributions of two carrier ensembles introduced in the formalism. This overlap is much stronger when the Pauli exclusion principle is included due to the additional statistical broadening. When degenerate statistics is taken into account, the Boltzmann equation is nonlinear, which makes its solution more difficult. One way to solve it is the well known method based on the Legendre polynomial expansion.[7] In this work, however, we employ the Monte Carlo approach.

We extend an approach presented in Ref. 4 for the small signal response analysis and construct a Monte Carlo algorithm for small signal analysis in degenerate semiconductors. We also clarify the physical aspects of the algorithm by considering the zero field limit and present a zero field mobility Monte Carlo algorithm, which in the limiting case of nondegenerate statistics gives the algorithm developed in Ref. 5.

The article is organized as follows. In Sec. II the Boltzmann kinetic equation including the Pauli exclusion principle is linearized. The integral form of the first order equation is constructed in Sec. III. The possibility of generating initial distributions for two particle ensembles is discussed in Sec. IV. In Sec. V we develop a combined rejection technique to solve the first order equation, and then the Monte Carlo algorithm is formulated. A physical interpretation of the method considering the zero field limit is given in Sec. VI. Next, the zero field Monte Carlo algorithm taking the Pauli exclusion principle into account is presented. Finally, results obtained for degenerate semiconductors are presented in Sec. VII.

II. LINEARIZED FORM OF THE BOLTZMANN EQUATION

We start from the Boltzmann kinetic equation, which takes the Pauli exclusion principle into account. The latter ensures that two electrons do not occupy the same quantum state. The case of a homogeneous bulk semiconductor is considered, and thus the space dependence of the distribution function is neglected. The differential scattering rates are assumed to be space and time invariant. With these conditions the Boltzmann equation takes the following form:

$$\frac{\partial f(\mathbf{k},t)}{\partial t} + \frac{q\mathbf{E}(t)}{\hbar} \cdot \nabla f(\mathbf{k},t) = Q[f](\mathbf{k},t), \tag{1}$$

[a]Electronic mail: smirnov@iue.tuwien.ac.at

 © 2003 American Institute of Physics

Downloaded 29 Oct 2003 to 128.130.68.74. Redistribution subject to AIP license or copyright, see http://ojps.aip.org/japo/japcr.jsp

with the scattering operator $Q[f](\mathbf{k},t)$ given by the expression:

$$Q[f](\mathbf{k},t)=\int f(\mathbf{k}',t)[1-f(\mathbf{k},t)]S(\mathbf{k}',\mathbf{k})d\mathbf{k}' - \int f(\mathbf{k},t)[1-f(\mathbf{k}',t)]S(\mathbf{k},\mathbf{k}')d\mathbf{k}'. \quad (2)$$

Here, $\mathbf{E}(t)$ is the electric field, q is the particle charge, and $S(\mathbf{k}',\mathbf{k})$ stands for the differential scattering rate.

In order to linearize Eq. (1), we write the electric field in the form

$$\mathbf{E}(t)=\mathbf{E}_s+\mathbf{E}_1(t), \quad (3)$$

where $\mathbf{E}_s$ denotes a stationary field and $\mathbf{E}_1(t)$ a small perturbation superimposed on the stationary field. It is assumed that this small perturbation of the electric field causes a small perturbation of the distribution function, which is written as follows:

$$f(\mathbf{k},t)=f_s(\mathbf{k})+f_1(\mathbf{k},t), \quad (4)$$

where $f_s(\mathbf{k})$ is a stationary distribution function and $f_1(\mathbf{k},t)$ a small deviation from the stationary distribution. Substituting Eq. (4) into Eq. (2), the scattering operator $Q[f](\mathbf{k},t)$ takes the form

$$Q[f](\mathbf{k},t)=\int [f_s(\mathbf{k}')+f_1(\mathbf{k}',t)] \times[1-f_s(\mathbf{k})-f_1(\mathbf{k},t)]S(\mathbf{k}',\mathbf{k})d\mathbf{k}' - \int [f_s(\mathbf{k})+f_1(\mathbf{k},t)][1-f_s(\mathbf{k}') - f_1(\mathbf{k}',t)]S(\mathbf{k},\mathbf{k}')d\mathbf{k}'. \quad (5)$$

Collecting terms of zero and first order we derive the zero order equation

$$\frac{q}{\hbar}\mathbf{E}_s\cdot\nabla f_s(\mathbf{k})=[1-f_s(\mathbf{k})]\int f_s(\mathbf{k}')S(\mathbf{k}',\mathbf{k})d\mathbf{k}' - f_s(\mathbf{k})\int [1-f_s(\mathbf{k}')]S(\mathbf{k},\mathbf{k}')d\mathbf{k}', \quad (6)$$

and the first order equation

$$\frac{\partial f_1(\mathbf{k},t)}{\partial t}+\frac{q}{\hbar}\mathbf{E}_s\cdot\nabla f_1(\mathbf{k},t)=-\frac{q}{\hbar}\mathbf{E}_1(t)\cdot\nabla f_s(\mathbf{k}) + Q_{(1)}[f](\mathbf{k},t), \quad (7)$$

where we have introduced the notation:

$$Q_1[f](\mathbf{k},t)=[1-f_s(\mathbf{k})]\int f_1(\mathbf{k}',t)S(\mathbf{k}',\mathbf{k})d\mathbf{k}' - f_1(\mathbf{k},t)\int [1-f_s(\mathbf{k}')]S(\mathbf{k},\mathbf{k}')d\mathbf{k}' - f_1(\mathbf{k},t)\int f_s(\mathbf{k}')S(\mathbf{k}',\mathbf{k})d\mathbf{k}' + f_s(\mathbf{k})\int f_1(\mathbf{k}',t)S(\mathbf{k},\mathbf{k}')d\mathbf{k}'. \quad (8)$$

Equation (7) is linear with respect to $f_1(\mathbf{k},t)$ and represents a kinetic equation, which differs from the usual form of the Boltzmann equation, whereas the stationary Boltzmann Eq. (6) is nonlinear with respect to $f_s(\mathbf{k})$. The differences of Eq. (7) from the conventional form of the Boltzmann equation are the additional term on the right-hand side proportional to $\mathbf{E}_1$ and the expression for the scattering operator, which has a more complex form. Both terms depend on the stationary distribution $f_s(\mathbf{k})$. Finally, it should be noted that in general both Eqs. (6) and (7) must be solved to find the response characteristics.

III. INTEGRAL REPRESENTATION OF THE BOLTZMANN-LIKE EQUATION

To construct a Monte Carlo algorithm we reformulate Eq. (7) as an integral equation. For this purpose we introduce a new differential scattering rate $\tilde{S}(\mathbf{k}',\mathbf{k})$ and a new total scattering rate $\tilde{\lambda}(\mathbf{k})$, respectively,

$$\tilde{S}(\mathbf{k}',\mathbf{k})=[1-f_s(\mathbf{k})]S(\mathbf{k}',\mathbf{k})+f_s(\mathbf{k})S(\mathbf{k},\mathbf{k}'), \quad (9)$$

$$\tilde{\lambda}(\mathbf{k})=\int \{[1-f_s(\mathbf{k}')]S(\mathbf{k},\mathbf{k}')+f_s(\mathbf{k}')S(\mathbf{k}',\mathbf{k})\}d\mathbf{k}' = \int \tilde{S}(\mathbf{k},\mathbf{k}')d\mathbf{k}'. \quad (10)$$

It is worth noting that the similarity with the standard Boltzmann equation is only formal, as both differential and total scattering rates are now functionals of the stationary distribution function, which is the solution of the equation of zero order (6).

With these definitions the scattering operator of the first order formally takes on the conventional form:

$$Q_1[f](\mathbf{k},t)=\int f_1(\mathbf{k}',t)\tilde{S}(\mathbf{k}',\mathbf{k})d\mathbf{k}'-f_1(\mathbf{k},t)\tilde{\lambda}(\mathbf{k}), \quad (11)$$

and the Boltzmann-like equation can be rewritten as follows:

$$\frac{\partial f_1(\mathbf{k},t)}{\partial t}+\frac{q}{\hbar}\mathbf{E}_s\cdot\nabla f_1(\mathbf{k},t) = \int f_1(\mathbf{k}',t)\tilde{S}(\mathbf{k}',\mathbf{k})d\mathbf{k}'-f_1(\mathbf{k},t)\tilde{\lambda}(\mathbf{k}) - \frac{q}{\hbar}\mathbf{E}_1(t)\cdot\nabla f_s(\mathbf{k}). \quad (12)$$

We derive the integral form of this equation using techniques described in Ref. 8. Introducing a phase space trajectory $\mathbf{K}(t')=\mathbf{k}-(q/\hbar)\mathbf{E}_s(t-t')$, which is the solution of Newton's equation, and taking into account that the perturbation is switched on at $t=0$, and thus $f_1[\mathbf{K}(t_0),t_0]=0$ for $t_0<0$, we obtain the following integral form:

Downloaded 29 Oct 2003 to 128.130.68.74. Redistribution subject to AIP license or copyright, see http://ojps.aip.org/japo/japcr.jsp

$$f_1[\mathbf{K}(t),t]=\int_0^t dt'\int d\mathbf{k}' f_1(\mathbf{k}',t')\tilde{S}[\mathbf{k}',\mathbf{K}(t')]\times\exp\left(-\int_{t'}^t\tilde{\lambda}[\mathbf{K}(y)]dy\right)-\frac{q}{\hbar}\int_0^t\mathbf{E}_1(t')\times[\nabla f_s][\mathbf{K}(t')]\cdot\exp\left(-\int_{t'}^t\tilde{\lambda}[\mathbf{K}(y)]dy\right)dt'. \tag{13}$$

Finally, we assume an impulse like excitation of the electric field, $\mathbf{E}_1(t)=\delta(t)\mathbf{E}_{\mathrm{im}}$, and obtain

$$f_1[\mathbf{K}(t),t]=\int_0^t dt'\int d\mathbf{k}' f_1(\mathbf{k}',t')\tilde{S}[\mathbf{k}',\mathbf{K}(t')]\times\exp\left(-\int_{t'}^t\tilde{\lambda}[\mathbf{K}(y)]dy\right)+G[\mathbf{K}(0)]\times\exp\left(-\int_0^t\tilde{\lambda}[\mathbf{K}(y)]dy\right), \tag{14}$$

where

$$G(\mathbf{k})=-\frac{q}{\hbar}\mathbf{E}_{\mathrm{im}}\cdot\nabla f_s(\mathbf{k}). \tag{15}$$

The essential difference of this integral representation from the one of the nondegenerate approach consists in the appearance of the new differential scattering rate $\tilde{S}(\mathbf{k}',\mathbf{k})$ and total scattering rate $\tilde{\lambda}(\mathbf{k})$. Another difference from the integral form of the Boltzmann equation for the nondegenerate case is common to both approaches and is reflected by the additional free term on the right-hand side, which in general cannot be treated as an initial distribution, because it can take on negative values.

IV. SOLUTION OF THE ZERO ORDER EQUATION

To solve the nonlinear Boltzmann equation including the Pauli exclusion principle Monte Carlo algorithms based on a rejection technique have been developed by Bosi and Jacoboni[9] and later by Lugli and Ferry.[10] We adopt the first algorithm to solve the zero order equation. In the following, we show that this algorithm can also be used to generate the initial distributions G^+ and G^- of the two carrier ensembles, which appear in the first order equation. The normalization of the stationary distribution required for the correct rejection is discussed.

A. Initial distributions of the two ensembles

Using the same method as suggested in Ref. 4, the free term in Eq. (14) is split into two positive functions G^+ and G^-, which are related to G through the relation: $G=G^+-G^-$. These two positive functions are considered as initial distributions of two carrier ensembles, which contain the same numbers of particles. To find the initial distributions for the case of a longitudinal perturbation we use the zero order Eq. (6), which gives together with Eq. (9):

$$G(\mathbf{k})=\frac{E_{\mathrm{im}}}{E_s}\cdot\left(\lambda(\mathbf{k})f_s(\mathbf{k})-\int f_s(\mathbf{k}')\tilde{S}(\mathbf{k}',\mathbf{k})d\mathbf{k}'\right), \tag{16}$$

where $\lambda(\mathbf{k})=\int S(\mathbf{k},\mathbf{k}')d\mathbf{k}'$. The last expression suggests splitting G into two positive functions. From the balance condition stated by the zero order Eq. (6) it follows $\langle\tilde{\lambda}\rangle_s=\langle\lambda\rangle_s$, where the stationary statistical average is defined as $\langle\cdots\rangle_s=\int f_s(\mathbf{k})\cdots d\mathbf{k}$. Then, the initial distributions can be written as

$$G^+=\frac{E_{\mathrm{im}}}{E_s}\langle\tilde{\lambda}\rangle_s\left\{\frac{\lambda(\mathbf{k})f_s(\mathbf{k})}{\langle\lambda\rangle_s}\right\},\qquad G^-=\frac{E_{\mathrm{im}}}{E_s}\langle\tilde{\lambda}\rangle_s\int\left\{\frac{\tilde{\lambda}(\mathbf{k})f_s(\mathbf{k})}{\langle\tilde{\lambda}\rangle_s}\right\}\left\{\frac{\tilde{S}(\mathbf{k},\mathbf{k}')}{\tilde{\lambda}(\mathbf{k})}\right\}d\mathbf{k}. \tag{17}$$

As can be seen from Eq. (17), G^+ represents the normalized before-scattering distribution function for a particle trajectory whose free-flight times are determined by the conventional scattering rate $\lambda(\mathbf{k})$, while G^- gives the normalized after-scattering distribution function for a particle trajectory constructed using $\tilde{S}(\mathbf{k},\mathbf{k}')$ and $\tilde{\lambda}(\mathbf{k})$, respectively.

B. Integral form of the nonlinear Boltzmann equation

To show how to generate the distributions G^+ and G^- we use the integral representation of the stationary Boltzmann Eq. (6). To accomplish this we first reformulate the scattering operator in Eq. (6):

$$Q[f_s]=[1-f_s(\mathbf{k})]\int f_s(\mathbf{k}')S(\mathbf{k}',\mathbf{k})d\mathbf{k}'+\int f_s(\mathbf{k}')\alpha(\mathbf{k}')\lambda(\mathbf{k}')\delta(\mathbf{k}-\mathbf{k}')d\mathbf{k}'-f_s(\mathbf{k})\times\left\{\int[1-f_s(\mathbf{k}')]S(\mathbf{k},\mathbf{k}')d\mathbf{k}'+\alpha(\mathbf{k})\lambda(\mathbf{k})\right\}, \tag{18}$$

where we have introduced the self-scattering rate $\alpha(\mathbf{k})$, and the delta function guarantees that the self-scattering does not change an electron state. Free-flight times are generated using the total scattering rate $\lambda(\mathbf{k})$ and we require the self-scattering rate to fulfill the equality

$$\lambda(\mathbf{k})=\int[1-f_s(\mathbf{k}')]S(\mathbf{k},\mathbf{k}')d\mathbf{k}'+\alpha(\mathbf{k})\lambda(\mathbf{k}). \tag{19}$$

This gives for the self-scattering rate the following expression:

$$\alpha(\mathbf{k})=\frac{1}{\lambda(\mathbf{k})}\int f_s(\mathbf{k}')S(\mathbf{k},\mathbf{k}')d\mathbf{k}'. \tag{20}$$

We introduce an additional differential scattering rate $\hat{S}(\mathbf{k},\mathbf{k}')$:

$$\hat{S}(\mathbf{k},\mathbf{k}')=[1-f_s(\mathbf{k}')]S(\mathbf{k},\mathbf{k}')+\alpha(\mathbf{k})\lambda(\mathbf{k})\delta(\mathbf{k}-\mathbf{k}'), \tag{21}$$

$$\int\frac{\hat{S}(\mathbf{k},\mathbf{k}')}{\lambda(\mathbf{k})}d\mathbf{k}'=1. \tag{22}$$

Downloaded 29 Oct 2003 to 128.130.68.74. Redistribution subject to AIP license or copyright, see http://ojps.aip.org/japo/japcr.jsp

Now, taking into account Eqs. (19) and (21), the scattering operator (18) takes the conventional form:

$$Q[f_s]=\int f_s(\mathbf{k}')\hat{S}(\mathbf{k}',\mathbf{k})d\mathbf{k}'-f_s(\mathbf{k})\lambda(\mathbf{k}). \tag{23}$$

Using the Neumann series of the forward equation we derive as an example the second iteration term as:[8]

$$\begin{aligned}f_\Omega^{(2)}=&\int_0^\infty dt_2\int_{t_2}^\infty dt_1\int_{t_1}^\infty dt_0\int d\mathbf{k}_2^a\int d\mathbf{k}_1^a\int d\mathbf{k}_i\cdot\{f_0(\mathbf{k}_i)\}\\&\times\left\{\exp\left(-\int_0^{t_2}\lambda[\mathbf{K}_2(y)]dy\right)\lambda[\mathbf{K}_2(t_2)]\frac{\hat{S}[\mathbf{K}_2(t_2),\mathbf{k}_2^a]}{\lambda[\mathbf{K}_2(t_2)]}\right\}\\&\times\left\{\exp\left(-\int_{t_2}^{t_1}\lambda[\mathbf{K}_1(y)]dy\right)\lambda[\mathbf{K}_1(t_1)]\frac{\hat{S}[\mathbf{K}_1(t_1),\mathbf{k}_1^a]}{\lambda[\mathbf{K}_1(t_1)]}\right\}\\&\times\left\{\exp\left(-\int_{t_1}^{t_0}\lambda[\mathbf{K}(y)]dy\right)\lambda[\mathbf{K}(t_0)]\right\}\\&\times\Theta(t-t_1)\Theta_\Omega[\mathbf{K}(t)]\Theta(t_0-t).\end{aligned} \tag{24}$$

Here the **k**-space is assumed to be divided in a mesh with the elementary volume $\Delta_{\mathbf{k}}$, $\Theta_\Omega(\mathbf{k})$ is the indicator defined as a function with values unity if $\mathbf{k}\in\Omega$ and zero otherwise, $\Theta(t)$ is the step function and $f_\Omega^{(2)}=\int f^{(2)}(\mathbf{k},t)\Theta_\Omega(\mathbf{k})d\mathbf{k}$. From Eq. (24) we see that if the free-flight time is calculated according to the scattering rate $\lambda(\mathbf{k})$, the conditional probability density for an after-scattering state $\mathbf{k}'$ from the initial state $\mathbf{k}$ is equal to $\hat{S}(\mathbf{k},\mathbf{k}')/\lambda(\mathbf{k})$.

Within the algorithm presented in Ref. 9 the before-scattering distribution function is equal to $\lambda(\mathbf{k})f_s(\mathbf{k})/\langle\lambda\rangle_s$, which gives the distribution G^+. In order to find the distribution function of the after-scattering states the before-scattering distribution function should be multiplied by the conditional probability density for an after-scattering state and this product is integrated over all before-scattering states. Using Eqs. (21) and (20) we obtain for the after-scattering distribution:

$$\begin{aligned}&\int\left\{\frac{\lambda(\mathbf{k})f_s(\mathbf{k})}{\langle\lambda\rangle_s}\right\}\left\{\frac{\hat{S}(\mathbf{k},\mathbf{k}')}{\lambda(\mathbf{k})}\right\}d\mathbf{k}\\&=\int\left\{\frac{\lambda(\mathbf{k})f_s(\mathbf{k})}{\langle\lambda\rangle_s}\right\}\frac{[1-f_s(\mathbf{k}')]S(\mathbf{k},\mathbf{k}')}{\lambda(\mathbf{k})}d\mathbf{k}\\&\quad+\frac{\lambda(\mathbf{k}')f_s(\mathbf{k}')}{\langle\lambda\rangle_s}\alpha(\mathbf{k}')\\&=\int\left\{\frac{\lambda(\mathbf{k})f_s(\mathbf{k})}{\langle\lambda\rangle_s}\right\}\frac{[1-f_s(\mathbf{k}')]S(\mathbf{k},\mathbf{k}')}{\lambda(\mathbf{k})}d\mathbf{k}\\&\quad+\int\left\{\frac{\lambda(\mathbf{k})f_s(\mathbf{k})}{\langle\lambda\rangle_s}\right\}\frac{f_s(\mathbf{k}')S(\mathbf{k}',\mathbf{k})}{\lambda(\mathbf{k})}d\mathbf{k}\\&=\int\left\{\frac{\tilde{\lambda}(\mathbf{k})f_s(\mathbf{k})}{\langle\tilde{\lambda}\rangle_s}\right\}\left\{\frac{\tilde{S}(\mathbf{k},\mathbf{k}')}{\tilde{\lambda}(\mathbf{k})}\right\}d\mathbf{k}=\frac{E_s}{E_{\mathrm{im}}\langle\tilde{\lambda}\rangle_s}G^-(\mathbf{k}'),\end{aligned} \tag{25}$$

which is normalized to unity. This means that we can generate initial distributions G^+ and G^- by introduction of the main trajectory, which is constructed using the algorithm from Ref. 9 to solve Eq. (6). Then, for each main iteration two carrier ensembles with initial distributions G^+ and G^- evolve in time according to Eq. (7) for the secondary trajectories.

C. Normalization of the stationary distribution function

The stationary distribution function $f_s(\mathbf{k})$ must be properly normalized as a probability, $0<f_s(\mathbf{k})<1$ to guarantee the correct rejection of scattering events. The **k** space is divided into subdomains Ω of size $V_\Omega=(\Delta k)^3$. In the following, $\overline{f}_\Omega$ stands for the average distribution function in Ω for a given valley and n is the contribution to the electron density from the same valley. In each subdomain the electron density is

$$n_\Omega=\frac{1}{4\pi^3}\int_\Omega f_s(\mathbf{k})d\mathbf{k}, \tag{26}$$

and the average distribution function is given as

$$\overline{f}_\Omega=\frac{\int_\Omega f_s(\mathbf{k})d\mathbf{k}}{V_\Omega}=\frac{4\pi^3 n_\Omega}{V_\Omega}. \tag{27}$$

Using the before-scattering estimation for the statistical average

$$\langle\langle A\rangle\rangle=C\frac{1}{N}\sum_b\frac{A(\mathbf{k}_b)}{\lambda(\mathbf{k}_b)}, \tag{28}$$

where N is the number of electron-free flights and the normalization constant C is given as

$$C=\frac{4\pi^3 N\cdot n}{\Sigma_b\dfrac{1}{\lambda(\mathbf{k}_b)}}, \tag{29}$$

we find for n_Ω:

$$\begin{aligned}n_\Omega&=\frac{1}{4\pi^3}\int\Theta_\Omega(\mathbf{k})f_s(\mathbf{k})d\mathbf{k}\\&=\frac{\langle\langle\Theta_\Omega\rangle\rangle}{4\pi^3}=n\cdot\frac{\Sigma_b\Theta_\Omega(\mathbf{k}_b)/\lambda(\mathbf{k}_b)}{\Sigma_b 1/\lambda(\mathbf{k}_b)},\end{aligned} \tag{30}$$

where the indicator function $\Theta_\Omega(\mathbf{k})$ of subdomain Ω has been introduced. Substituting Eq. (30) into Eq. (27) we finally obtain for the average distribution function:

$$\overline{f}_\Omega=\frac{4\pi^3 n}{V_\Omega}\cdot\frac{\Sigma_b\Theta_\Omega(\mathbf{k}_b)/\lambda(\mathbf{k}_b)}{\Sigma_b 1/\lambda(\mathbf{k}_b)}. \tag{31}$$

V. SOLUTION OF THE FIRST ORDER EQUATION

Equation (7) contains terms that depend on the stationary distribution function $f_s(\mathbf{k})$. These are the free and scattering terms. The stationary distribution function is the solution of Eq. (6) and its shape can be arbitrary. This fact prevents an analytical solution for $\tilde{\lambda}$, and a numerical integration is necessary. However, in this work we apply a rejection technique

Downloaded 29 Oct 2003 to 128.130.68.74. Redistribution subject to AIP license or copyright, see http://ojps.aip.org/japo/japcr.jsp

to solve Eq. (7). In Sec. III we have introduced a new differential scattering rate $\tilde{S}$ [see Eq. (9)], and now we define another differential scattering rate according to the following expression:

$$\tilde{S}_0(\mathbf{k}',\mathbf{k}) = S(\mathbf{k}',\mathbf{k}) + S(\mathbf{k},\mathbf{k}'). \tag{32}$$

The corresponding total scattering rate is

$$\tilde{\lambda}_0(\mathbf{k}) = \lambda(\mathbf{k}) + \lambda^*(\mathbf{k}), \tag{33}$$

where λ^* stands for the total backward-scattering rate

$$S^*(\mathbf{k},\mathbf{k}') = S(\mathbf{k}',\mathbf{k}),$$
$$\lambda^*(\mathbf{k}) = \int S^*(\mathbf{k},\mathbf{k}')d\mathbf{k}'. \tag{34}$$

From Eqs. (9) and (32) it follows that

$$\tilde{S}_0(\mathbf{k}',\mathbf{k}) \geqslant \tilde{S}(\mathbf{k}',\mathbf{k}). \tag{35}$$

To solve Eq. (7) we generate a wave vector $\mathbf{k}$ using the differential scattering rate $S_0(\mathbf{k}',\mathbf{k})$. The condition of acceptance takes the following form:

$$r \cdot \tilde{S}_0(\mathbf{k}',\mathbf{k}) < \tilde{S}(\mathbf{k}',\mathbf{k}), \tag{36}$$

where r is a random number evenly distributed between 0 and 1. The last inequality may be rewritten as follows:

$$r \cdot [S(\mathbf{k}',\mathbf{k}) + S(\mathbf{k},\mathbf{k}')] < [1 - f_s(\mathbf{k})]S(\mathbf{k}',\mathbf{k}) + f_s(\mathbf{k})S(\mathbf{k},\mathbf{k}'). \tag{37}$$

Let us consider some special cases of the last inequality when the scattering process can be split into the sum of the emission and absorption of some quasiparticles (phonons, plasmons, etc.). Then, considering a forward transition from $\mathbf{k}'$ to $\mathbf{k}$ it can be easily shown that one of the following rejection conditions has to be checked depending on whether an absorption or emission process has occurred. For absorption processes it takes the form:

$$r \cdot \left[1 + \frac{N_{\mathrm{eq}}}{N_{\mathrm{eq}}+1}\right] < [1 - f_s(\mathbf{k})]\frac{N_{\mathrm{eq}}}{N_{\mathrm{eq}}+1} + f_s(\mathbf{k}), \tag{38}$$

whereas for emission processes we check

$$r \cdot \left[1 + \frac{N_{\mathrm{eq}}}{N_{\mathrm{eq}}+1}\right] < 1 - f_s(\mathbf{k}) + f_s(\mathbf{k})\frac{N_{\mathrm{eq}}}{N_{\mathrm{eq}}+1}, \tag{39}$$

where N_{eq} denotes the equilibrium number of quasiparticles. For example, when $N_{\mathrm{eq}}/(N_{\mathrm{eq}}+1) \ll 1$ we obtain from Eqs. (38) and (39) that for the nondegenerate case, $f_s \ll 1$, emission processes will be dominantly accepted while absorption processes will be mostly rejected. This means that the kinetic behavior is determined by emission processes. On the other side for the degenerate case, when $f_s \sim 1$, it follows from the same relations that emission processes will be mostly rejected while the probability of the acceptance of absorption processes increases. Finally, it should be noted that for elastic processes $[S(\mathbf{k},\mathbf{k}') = S(\mathbf{k}',\mathbf{k})]$ the rejection condition (37) takes the following form:

$$r < \tfrac{1}{2}. \tag{40}$$

This means that one half of the elastic scattering events will not be accepted in the rejection scheme given above.

Using Eq. (17) and the combined rejection technique developed for the secondary trajectories [see inequalities (38)–(40)], the new small-signal Monte Carlo algorithm including the Pauli exclusion principle can be formulated as follows:

(1) Simulate the nonlinear Boltzmann equation until f_s has converged.
(2) Follow a main trajectory for one free flight. Store the before-scattering state in $\mathbf{k}_b$, and realize a scattering event from $\mathbf{k}_b$ to $\mathbf{k}_a$.
(3) Start a trajectory $\mathbf{K}^+(t)$ from $\mathbf{k}_b$ and another trajectory $\mathbf{K}^-(t)$ from $\mathbf{k}_a$.
(4) Follow both trajectories for time T using the rejection scheme based on the acceptance conditions (38)–(40). At equidistant times t_i add $A[\mathbf{K}^+(t_i)]$ to a histogram α_i^+ and $A[\mathbf{K}^-(t_i)]$ to a histogram α_i^-.
(5) Continue with the second step until N $\mathbf{k}$ points have been generated.
(6) Calculate the time discrete impulse response as $\langle A \rangle_{\mathrm{im}}(t_i) = (E_{\mathrm{im}}\langle\lambda\rangle/NE_s)(\alpha_i^+ - \alpha_i^-)$.

VI. ZERO ELECTRIC FIELD LIMIT AND PHYSICAL INTERPRETATION OF THE METHOD

As mentioned in the previous section, in highly degenerate semiconductors the kinetic behavior can reverse and the backward processes will dominate over the forward ones. This effect can be more clearly explained by considering the zero electric field limit of the theory constructed above.

When the electric field tends to zero, the equilibrium distribution function can be assumed and represented by the Fermi–Dirac (FD) distribution function in the case of particles with fractional spin:

$$f_{\mathrm{FD}}(\epsilon) = \frac{1}{\exp\left[-\dfrac{E_f - \epsilon}{k_B T_0} + 1\right]}, \tag{41}$$

where E_f denotes the Fermi energy, ϵ stands for an electron energy, and T_0 is the equilibrium temperature equal to the lattice temperature. Since the stationary distribution is known, it is not necessary to solve the zero order Eq. (6). As can be seen from Eq. (41), in equilibrium the distribution function depends directly on the carrier energy and only indirectly on the wave vector through the $\epsilon(\mathbf{k})$ relation. This fact allows us to significantly simplify Eq. (10) using the Fermi golden rule:[11]

$$S(\mathbf{k},\mathbf{k}') = \frac{V}{4\pi^2\hbar}|V_{fi}|^2 \delta[\epsilon(\mathbf{k}') - \epsilon(\mathbf{k}) \pm \Delta\epsilon]. \tag{42}$$

Making use of the delta function in the last expression and assuming the independence of V_{fi} and $\Delta\epsilon$ from $\mathbf{k}$ and $\mathbf{k}'$, we rewrite Eq. (10) in the following manner:

$$\tilde{\lambda}(\mathbf{k}) = [1 - f_{\mathrm{FD}}(\epsilon_f)]\lambda(\mathbf{k}) + f_{\mathrm{FD}}(\epsilon_f)\lambda^*(\mathbf{k}), \tag{43}$$

Downloaded 29 Oct 2003 to 128.130.68.74. Redistribution subject to AIP license or copyright, see http://ojps.aip.org/japo/japcr.jsp

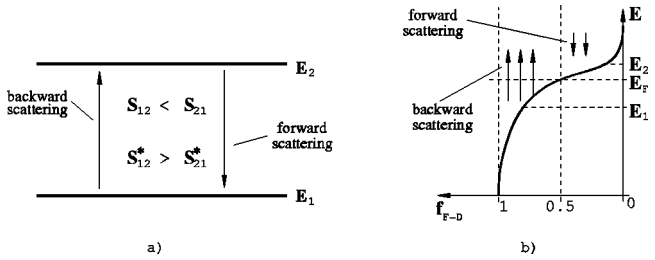

FIG. 1. Schematic illustration of the scattering processes at high degeneracy.

where ϵ_f denotes the final carrier energy. Equation (43) represents a linear combination of the total forward- and backward-scattering rates.

In the nondegenerate case, $f_{\mathrm{FD}}(\epsilon) \ll 1$, we obtain $\tilde{\lambda}(\mathbf{k}) = \lambda(\mathbf{k})$, which means that the scattering processes are mostly determined by the forward-scattering rate, and thus the algorithm developed in Ref. 5 for nondegenerate statistics is restored. On the other hand, for highly degenerate semiconductors, $f_{\mathrm{FD}}(\epsilon) \sim 1$, the scattering processes are dominantly backward $\tilde{\lambda}(\mathbf{k}) = \lambda^*(\mathbf{k})$. In the case of intermediate degeneracy both forward and backward scattering contributes to the kinetics.

The fact that backward scattering is dominant in processes where an initial state of an electron has lower energy than in its final state can formally be explained from the point of view of the principle of detailed balance given by the symmetry relation

$$S(\mathbf{k},\mathbf{k}') \cdot \exp\left(\frac{\epsilon(\mathbf{k}')}{k_B T_0}\right) = S^*(\mathbf{k},\mathbf{k}') \cdot \exp\left(\frac{\epsilon(\mathbf{k})}{k_B T_0}\right). \qquad (44)$$

As can be seen from Eq. (44), forward transitions from high to low energy levels are preferred, and backward transitions from low to high energy levels prevail.

It should be mentioned that at high degeneracy the backward scattering rate is dominant, and thus the probability of scattering to higher energy levels is larger than to lower energy levels, as schematically shown in Fig. 1(a). Physically, this means that lower energy levels are already occupied by particles, $f_{\mathrm{FD}}(\epsilon) \approx 1$ [see Fig. 1(b)] and, due to the Pauli exclusion principle, scattering to these energy levels is quantum mechanically forbidden.

Using the approach described in this section, a zero field Monte Carlo algorithm including the Pauli exclusion principle[12] has been constructed, which gives the whole mobility tensor in semiconductors with an arbitrary level of degeneracy:

(1) Set $n=0$, $w=0$,
(2) select initial state $\mathbf{k}$ arbitrarily,
(3) compute a sum of weights: $w = w + [1 - f_{\mathrm{FD}}(\epsilon)] \times [v_j(\mathbf{k})/\tilde{\lambda}(\mathbf{k})]$,
(4) select a free-flight time $\tilde{t}_f = -\ln(r)/\tilde{\lambda}(\mathbf{k})$ and add time integral to estimator: $n = n + w v_i \tilde{t}_f$, or use the expected value of the time integral: $n = n + w[v_i/\tilde{\lambda}(\mathbf{k})]$.

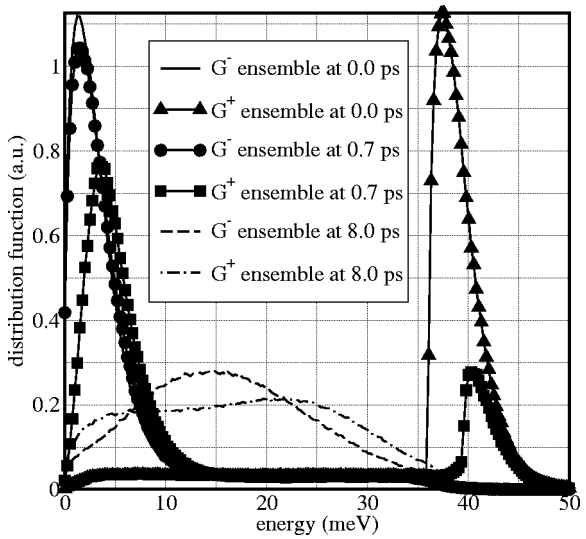

FIG. 3. Energy distribution functions for the two carrier ensembles in GaAs. Low electron density: $n = 10^{14}$ cm^{-3}.

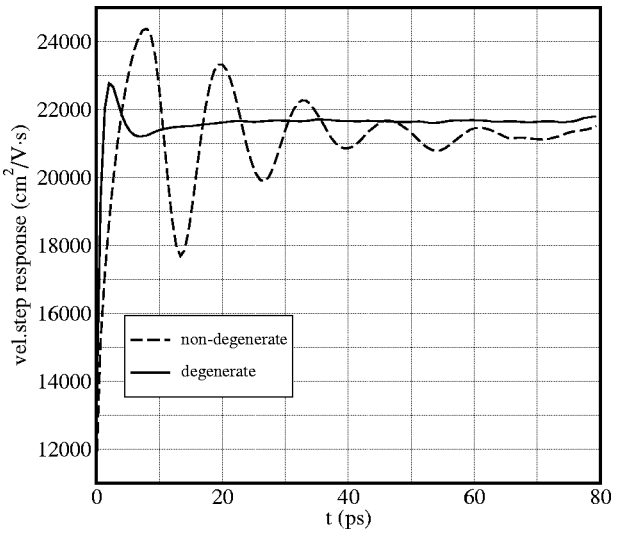

FIG. 2. Velocity step response in degenerate ($n = 10^{18}$ cm^{-3}) GaAs. $E_s = 120$ V/cm.

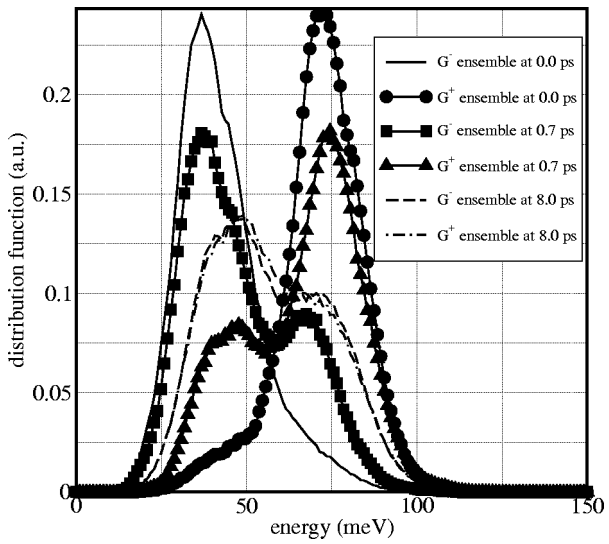

FIG. 4. Energy distribution functions for the two carrier ensembles in GaAs. High electron density: $n = 10^{18}$ cm^{-3}.

Downloaded 29 Oct 2003 to 128.130.68.74. Redistribution subject to AIP license or copyright, see http://ojps.aip.org/japo/japcr.jsp

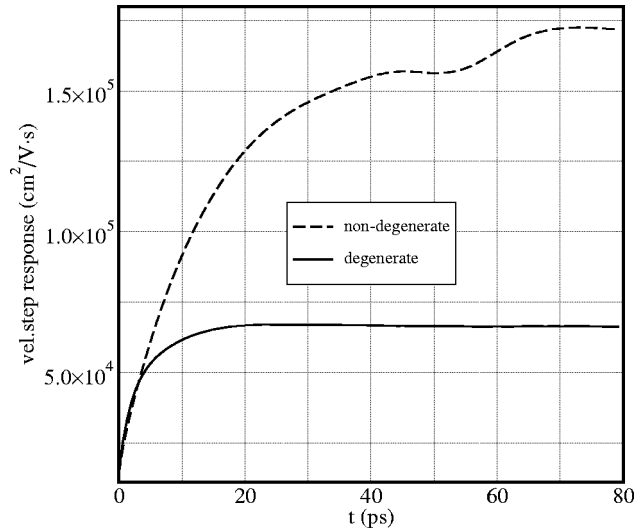

FIG. 5. Velocity step response in degenerate ($n=10^{18}$ cm^{-3}) GaAs. $E_s=30$ V/cm.

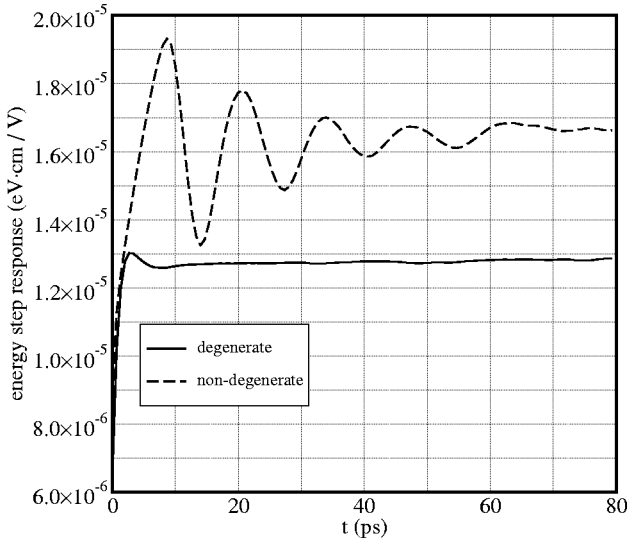

FIG. 7. Energy step response in degenerate ($n=10^{18}$ cm^{-3}) GaAs. $E_s=120$ V/cm.

(5) perform scattering. If the mechanism was isotropic, reset weight: $w=0$,
(6) continue with step (3) until N **k** points have been generated,
(7) calculate component of zero field mobility tensor as $\mu_{ij}=q\langle\tilde{\lambda}\rangle n/(k_B T_0 N)$.

In step (5) we use the fact that time integration can be stopped after the first velocity randomizing scattering event has occurred, because in this case the correlation of the trajectory's initial velocity with the after-scattering velocity is lost.

VII. RESULTS

For our Monte Carlo simulations we only consider electrons in the first conduction band, which is described by an analytical model[13,14] including nonparabolicity and anisotropy. Scattering on phonons includes both intravalley and intervalley transitions. Acoustic phonons are treated as an elastic mechanism.

First, we present simulations for GaAs at 25 K to demonstrate the transit time resonance effect in the nondegenerate material and its behavior in the case of high degeneracy. In Fig. 2 we show the velocity step response at an electric field $E_s=120$ V/cm, electron density $n=10^{18}$ cm^{-3}, and the influence of the Pauli exclusion principle. It can be seen that when degeneracy is taken into account, the oscillations are suppressed. On the other hand, the stationary values are nearly the same for both algorithms. The significant reduction of the oscillations can be explained in terms of the energy distribution functions shown in Figs. 3 and 4 for both cases. Under degenerate conditions the distribution functions overlap much stronger due to the exclusion principle. The

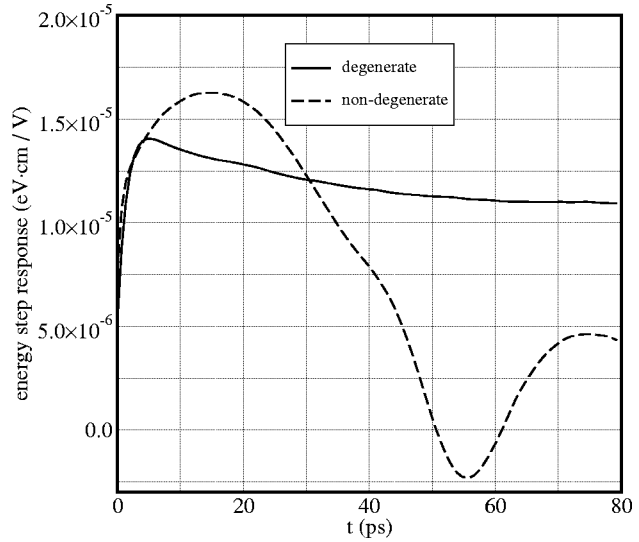

FIG. 6. Energy step response in degenerate ($n=10^{18}$ cm^{-3}) GaAs. $E_s=30$ V/cm.

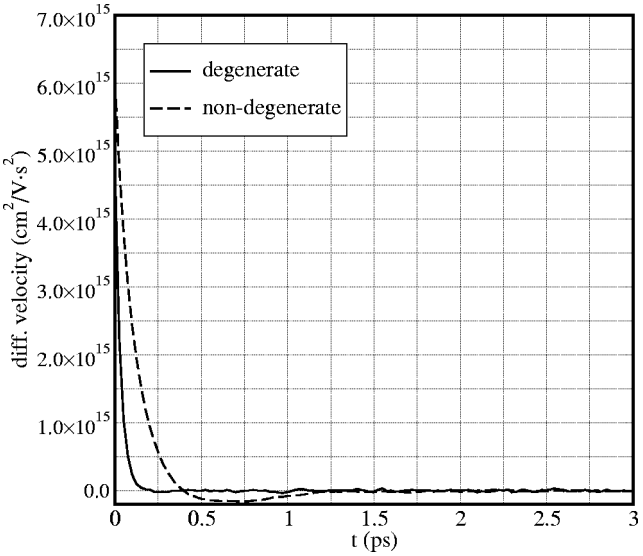

FIG. 8. Differential velocity in degenerate ($n=10^{21}$ cm^{-3}) Si. $E_s=5000$ V/cm.

Downloaded 29 Oct 2003 to 128.130.68.74. Redistribution subject to AIP license or copyright, see http://ojps.aip.org/japo/japcr.jsp

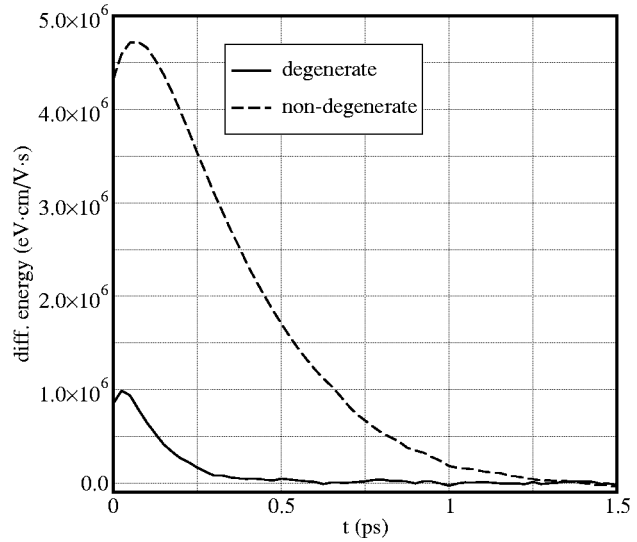

FIG. 9. Differential energy in degenerate ($n=10^{21}$ cm^{-3}) Si. E_s $=5000$ V/cm.

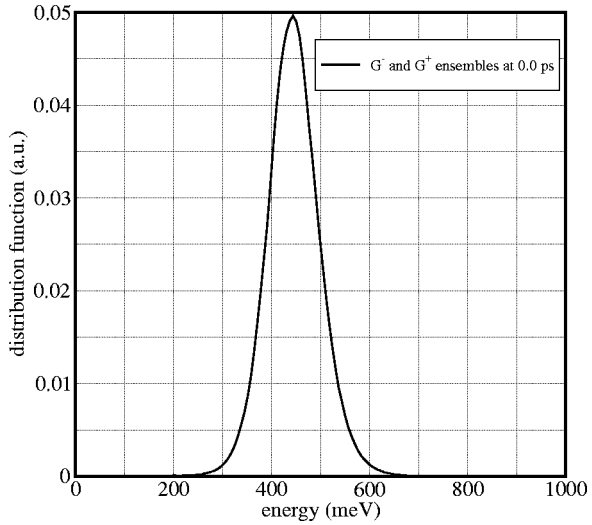

FIG. 11. Energy distribution functions for the two carrier ensembles in Si. High electron density: $n=10^{21}$ cm^{-3}.

difference between the two ensembles disappears faster in the case when the Pauli principle is considered. As the impulse response is equal to the difference of the mean values of the two ensembles, it explains the weaker oscillations in the degenerate case. The small difference of the stationary values is related to the high absolute value of the electric field. In Fig. 5 it is shown that this difference is more significant at a lower absolute value of the electric field E_s $=30$ V/cm. Figures 6 and 7 demonstrate the energy step response at $E_s=30$ V/cm and $E_s=120$ V/cm, respectively.

As a second example we present results for Si at 300K, $E_s=5$ kV/cm, $n=10^{21}$ cm^{-3}. Figures 8 and 9 show the differential velocity and differential energy, respectively. The differential velocity obtained from the nondegenerate algorithm displays a weak oscillatory character, while the differential velocity obtained by the degenerate algorithm does not show any oscillations. This again can be explained analyzing the energy distribution functions. The small difference of the distribution functions of the two ensembles in the nondegenerate algorithm (see Fig. 10) is responsible for the weak oscillation, while for the degenerate algorithm the two ensembles have the same distributions at the very beginning, as is shown in Fig. 11. In addition, in the degenerate case the distribution functions significantly shift to higher energies as the lower energy levels are occupied and scattering to these states is forbidden.

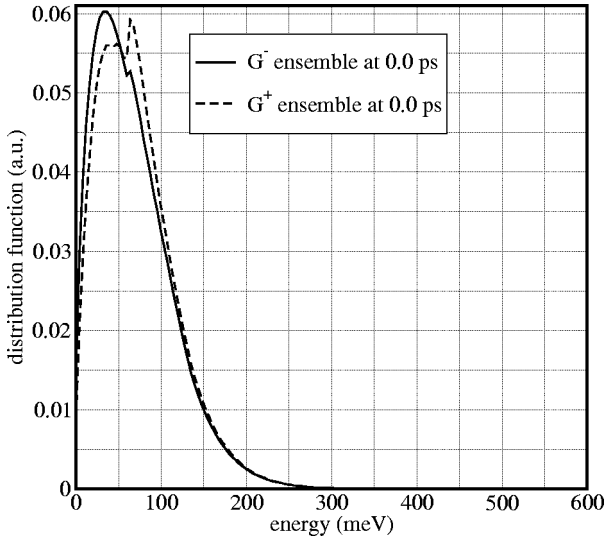

FIG. 10. Energy distribution functions for the two carrier ensembles in Si. Low electron density: $n=10^{14}$ cm^{-3}.

VIII. CONCLUSION

A Monte Carlo algorithm for small-signal analysis including the quantum mechanical Pauli exclusion principle has been presented. The original nonlinear Boltzmann equation has been split into two equations. To obtain the stationary distribution and the initial distributions for the two carrier ensembles the algorithm of Bosi and Jacoboni[9] has been applied. To solve the first order equation a combined rejection technique has been developed. The physical essence of the algorithm has been clarified by considering the zero electric field limit. It has been shown that the Pauli exclusion principle reverses the carrier kinetics in highly degenerate semiconductors. Finally, some results of the small-signal analysis have been presented for highly degenerate semiconductors.

[1] P. Price, J. Appl. Phys. **54**, 3616 (1983).
[2] E. Starikov, P. Shiktorov, V. Gružinskis, L. Varani, J. Vaissiere, J. Nougier, and L. Reggiani, J. Appl. Phys. **79**, 242 (1996).
[3] M. Nedjalkov, H. Kosina, and S. Selberherr, in SISPAD, Kyoto, Japan (1999), pp. 155–158.
[4] H. Kosina, M. Nedjalkov, and S. Selberherr, J. Appl. Phys. **87**, 4308 (2000).
[5] H. Kosina, M. Nedjalkov, and S. Selberherr, in *Large-Scale Scientific Computing, Sozopol, Bulgaria* (Springer, Berlin, 2001), pp. 175–182.
[6] L. Reggiani, E. Starikov, P. Shiktorov, V. Gružinskis, and L. Varani, Semicond. Sci. Technol. **12**, 141 (1997).
[7] H. Lin and N. Goldsman, Solid-State Electron. **34**, 1035 (1991).
[8] H. Kosina, M. Nedjalkov, and S. Selberherr, IEEE Trans. Electron Devices **47**, 1898 (2000).
[9] S. Bosi and C. Jacoboni, J. Phys. C **9**, 315 (1976).

Downloaded 29 Oct 2003 to 128.130.68.74. Redistribution subject to AIP license or copyright, see http://ojps.aip.org/japo/japcr.jsp

[10] P. Lugli and D. K. Ferry, IEEE Trans. Electron Devices **32**, 2431 (1985).
[11] L. D. Landau and E. M. Lifshitz, *Quantum Mechanics: Nonrelativistic Theory* (Butterworth-Heinemann, Washington, DC, 1981).
[12] S. Smirnov, H. Kosina, M. Nedjalkov, and S. Selberherr, in *Large-Scale Scientific Computing, Sozopol, Bulgaria* (Springer, Berlin, 2003).
[13] C. Jacoboni and L. Reggiani, Rev. Mod. Phys. **55**, 645 (1983).
[14] C. Jacoboni and P. Lugli, *The Monte Carlo Method for Semiconductor Device Simulation* (Springer, Wien, 1989).

Downloaded 29 Oct 2003 to 128.130.68.74. Redistribution subject to AIP license or copyright, see http://ojps.aip.org/japo/japcr.jsp